Special Issue Article

Journal of PeptideScience

Received: 25 October 2012 Revised: 8 January 2013 Accepted: 10 January 2013 Published online in Wiley Online Library: 19 February 2013

(wileyonlinelibrary.com) DOI 10.1002/psc.2487

Analysis of the haptoglobin binding region on the apolipoprotein A-I-derived P2a peptide‡

Maria Stefania Spagnuolo,[a§] Rossella Di Stasi,[b§] Lucia De Rosa,[b] Bernadetta Maresca,[c] Luisa Cigliano[c] and Luca D. D'Andrea[b]*

Apolipoprotein A-I (ApoA-I) is the main protein component of the high density lipoproteins and it plays an important role in the reverse cholesterol transport. In particular, it stimulates cholesterol efflux from peripheral cells toward liver and activates the enzyme lecithin-cholesterol acyltransferase (LCAT). Haptoglobin (Hpt), a plasma α_2-glycoprotein belonging to the family of acute-phase proteins, binds to ApoA-I inhibiting the stimulation of the enzyme LCAT. Previously, we reported that a synthetic peptide, P2a, binds to and displaces Hpt from ApoA-I restoring the LCAT cholesterol esterification activity in the presence of Hpt. Here, we investigate the molecular determinants underlining the interaction between Hpt and P2a peptide. Analysis of truncated P2a analogs showed that P2a sequence can only be slight reduced in length at the *N*-terminal to preserve the ability of binding to Hpt. Binding assays showed that charged residues are not involved in Hpt recognition; actually, E146A and D157A substitutions increase the binding affinity to Hpt. Biological characterization of the corresponding P2a peptide analogs, Apo146 and Apo157, showed that the two peptides interfere with Hpt binding to HDL and are more effective than P2a peptide in rescue LCAT activity from Hpt inhibition. This result suggests novel hints to design peptides with anti-atherogenic activity. Copyright © 2013 European Peptide Society and John Wiley & Sons, Ltd.

Keywords: haptoglobin; ApoA-I; HDL; helix conformation; LCAT

Introduction

Apolipoprotein A-I (ApoA-I), the major protein component of the high density lipoproteins (HDL), plays an important role in the reverse cholesterol transport (RCT). It stimulates the efflux of cholesterol from peripheral cells toward liver and activates the enzyme lecithin-cholesterol acyltransferase (LCAT; EC 2.3.1.43) to convert cell-derived cholesterol into cholesteryl ester for HDL mediated transport to liver for excretion [1]. ApoA-I is composed of 243 amino acids organized in ten α-helix segments divided in eight 22-mer and two 11-mer repeats with a predominant amphipathic character. The structure of ApoA-I has been deeply investigated using several experimental techniques. These studies showed that ApoA-I is a dynamic protein characterized by structural plasticity depending on the lipid composition of HDL [2–8].

We previously reported that ApoA-I binds to Haptoglobin (Hpt) [9,10]. Hpt is a plasma α_2-glycoprotein, mainly expressed in the liver, belonging to the family of acute-phase proteins. Hpt binds free Hemoglobin (Hb) with extremely high affinity [11–13], and the complex is then caught by macrophages and hepatocytes for elimination from circulation [13,14]. In this way, Hpt prevents iron loss and represents the primary defense mechanism against free Hb [15,16]. Furthermore, Hpt protects ApoA-I against hydroxyl radicals, thus saving the apolipoprotein function in physiological conditions [17]. On the other hand, high levels of Hpt, as those circulating during inflammation, impair ApoA-I stimulation of both LCAT [9,10] and cholesterol uptake by hepatocytes [18]. Thereby, cholesterol removal from peripheral cells would be hampered, suggesting that high levels of Hpt, as present during the acute phase of inflammation, may play a critical role in worsening vascular endothelial dysfunction and accelerating atherosclerosis. Indeed, several studies have confirmed that high levels of Hpt are associated with increased risk of developing cardiovascular events or myocardial infarction [19–21].

We mapped the Hpt binding site on ApoA-I region 141–164, which overlaps with the ApoA-I domain required for LCAT stimulation [22]. This suggests that Hpt impairs LCAT activity by masking the stimulatory region of ApoA-I. Furthermore, we showed that a synthetic peptide, P2a, reproducing the ApoA-I sequence 141–164, binds to and displaces Hpt from ApoA-I on HDL surface [23]. The peptide P2a was able to restore the LCAT cholesterol esterification activity in the presence of Hpt *in vitro* [23] and *in vivo* in an experimental model of inflammation [24]. These results indicate that P2a effectively targets the Hpt–HDL recognition surface and suggest that P2a could be a promising candidate to modulate pharmaceutically the RCT.

In this context, we aim to investigate the molecular determinants underlining the interaction between Hpt and P2a peptide. In this work, we synthesized, characterized by CD spectroscopy and analyzed the biological properties of a series of P2a peptide analogs in order to address either the effect of peptide length and the role of charged residues. Finally, we selected two single amino acid substitutions which improved the biological activity of P2a.

* *Correspondence to: Luca Domenico D'Andrea, Istituto di Biostrutture e Bioimmagini, CNR, Via Mezzocannone 16, 80134, Napoli, Italy. E-mail: ldandrea@unina.it*

‡ *Special issue devoted to contributions presented at the 13th Naples Workshop on Bioactive Peptides, June 7-10, 2012, Naples.*

§ *These two authors contributed equally.*

a *Istituto per il Sistema Produzione Animale in Ambiente Mediterraneo, CNR, via Argine 1085, Napoli, Italy*

b *Istituto di Biostrutture e Bioimmagini, CNR, Via Mezzocannone 16, Napoli, Italy*

c *Dipartimento delle Scienze Biologiche, Università di Napoli 'Federico II', Via Mezzocannone 8, Napoli, Italy*

Journal of PeptideScience

Materials and Methods

Chemicals

Fmoc protected amino acids and coupling reagents were purchased from Inbios (Naples, Italy). PAL-PEG PS (Peptide Amide Linker – polyethylene glycol-polystyrene) resin was obtained from Perseptive Biosystem GmbH (Hamburg, Germany). Peptide synthesis solvents with the lowest water content (DMF, NMP (N-Methyl-2-pyrrolidone), and DCM) and acetonitrile were supplied by Romil (Cambridge, UK) and used without further purification; DIPEA, acetic anydride, piperidine, TIS (triisopropylsilane), diethyl ether, and HPLC solvents were from Sigma-Aldrich (Milan, Italy).

Biochemicals

Chemicals of the highest purity, fraction V BSA, human serum albumin, cholesterol, human Hpt (mixed phenotypes: Hpt 1–1, Hpt 1–2, and Hpt 2–2), rabbit anti-human Hpt IgG, goat anti-rabbit horseradish peroxidase-conjugated, *o*-phenylenediamine, Avidin-HRP, and molecular weight markers were purchased from Sigma-Aldrich (Milan, Italy). Human HDL was from Merck Millipore (Darmstadt, Germany). [1α,2α-^{3}H] Cholesterol (45 Ci/mmol) was obtained from Perkin Elmer (Boston, USA). Polystyrene 96-wells plates from Nunc (Roskilde, Denmark) and Sil-G plates for thin-layer chromatography (0.25 mm thickness) of Macherey-Nagel (Düren, Germany) were used. Sephacryl S-200, Blue Sepharose 6 Fast Flow, and CNBr-activated Sepharose were purchased from GE Healthcare Europe GmbH (Milan, Italy).

Solid Phase Peptide Synthesis

Peptides were synthesized on PAL-PEG PS resin (0.42 mmol/g) using standard Fmoc/tBu chemistry. Fmoc deprotection was performed washing the resin two times (7 min) with a solution of 30% piperidine in DMF, coupling reactions were performed with 8 equiv of Fmoc-amino acid and 7.9 HBTU/HOBt, 16 eq DIPEA in DMF for 45 min at room temperature, capping step (1 × 5 min) was performed with a solution of acetic anhydride (0.5 M)/HOBt (0.015 M)/DIPEA (0.125 M) in DMF. Each step was followed by five washing with DMF for 1 min. Peptides were biotinylated on solid phase reacting the peptide N^{α} amino group, after Fmoc deprotection, with 2 equiv of *N*-(+)-biotinyl-6-aminocaproic acid (Sigma-Aldrich, Milan, Italy), 2 equiv of HATU and 4 equiv of DIPEA in DMF o.n. at room temperature under shaking.

Peptide cleavage was performed using TFA/TIS/H_2O/EDT (94 : 1 : 2.5 : 2.5; v/v/v/v). Peptides were precipitated in cold ether and liophilyzed.

Peptide Purification and Analysis

Peptide purifications were carried out on a Shimadzu LC-8A, equipped with an SPD-M10 AV detector, using a C18 column Jupiter (250 × 10 mm, 300 Å, 10 μm; Phenomenex, Torrance, USA). Peptide identification was performed on the LC-MS Finnegan Surverior Thermo C (Thermo Fisher Scientific, Waltham, USA) equipped with an ESI source and single quadrupole mass analyzer coupled to a Surveyor HPLC system (with photo diode array detector) using a C18 column Jupiter (250 × 4.6 mm, 300 Å, 5 μm; Phenomenex, Torrance, USA). Peptide analytical characterization was carried out on a Hewlett Packard HP1100 HPLC equipped with UV detector using a C18 column Jupiter (250 × 4.6 mm, 300 Å, 5 μm; Phenomenex, Torrance, USA). Linear gradients of CH_3CN (0.1% TFA) in H_2O (0.1% TFA) at a flow rate of 1 ml/min were used in peptide analyses as reported below (5-70-30: from 5% to 70% over 30 min). All peptides were afforded in high pure and homogenous forms as assessed by analytical RP-HPLC (>95%-based chromatographic profile revealed at 210 nm).

Peptide P2a: MS *m/z* calcd 2756.3 Da, found 2757.2 Da, RP-HPLC R_t = 13.4 min (20-80-40); biotinylated MS *m/z* calcd, 3052.6 Da, found 3050.6 Da, RP-HPLC R_t = 16.0 min (5-70-30).

Peptide Apo146: MS *m/z* calcd, 2700.9 Da, found 2704.2 Da, RP-HPLC R_t = 17.1 min (5-70-25); biotinylated MS *m/z* calcd, 2996.9 Da, found 2998.4 Da, RP-HPLC R_t = 18.3 min (5-70-25).

Peptide Apo147: MS *m/z* calcd 2700.9 Da, found 2698.6 Da, RP-HPLC R_t = 17.0 min (5-70-25); biotinylated MS *m/z* calcd 2996.9 Da, found 2997.5 Da, RP-HPLC R_t = 24.6 min (5-70-30).

Peptide Apo149: MS *m/z* calcd 2673.9 Da, found 2670.6 Da, RP-HPLC R_t = 17.6 min (5-70-25); biotinylated MS *m/z* calcd 2969.9 Da, found 2970.2 Da, RP-HPLC R_t = 23.8 min (5-70-30).

Peptide Apo150: MS *m/z* calcd 2714.9 Da, found 2711.1 Da, RP-HPLC R_t = 16.8 min (5-70-25); biotinylated MS *m/z* calcd 3010.9 Da, found 3010.1 Da, RP-HPLC R_t = 24.8 min (5-70-25).

Peptide Apo151: MS *m/z* calcd 2673.9 Da, found 2671.2 Da, RP-HPLC R_t = 17.8 min (5-70-25); biotinylated MS *m/z* calcd 2969.9 Da, found 2970.5 Da, RP-HPLC R_t = 25.5 min (5-70-30).

Peptide Apo153: MS *m/z* calcd 2673.9 Da, found 2670.8 Da, RP-HPLC R_t = 17.4 min (5-70-25); biotinylated MS *m/z* calcd 2969.9 Da, found 2970.5 Da, RP-HPLC R_t = 22.5 min (5-70-30).

Peptide Apo155: MS *m/z* calcd 2692.9 Da, found 2688.0 Da, RP-HPLC R_t = 19.0 min (5-70-30); biotinylated MS *m/z* calcd 2988.9 Da, found 2987.3 Da, RP-HPLC R_t = 21.3 min (5-70-30).

Peptide Apo157: MS *m/z* calcd 2714.9 Da, found 2712.2 Da, RP-HPLC R_t = 17.0 min (5-70-25); biotinylated MS *m/z* calcd 3011.0 Da; found 3009.6 Da, RP-HPLC R_t = 23.0 min (5-70-30).

Peptide Apo160: MS *m/z* calcd 2673.9 Da, found 2671.2 Da, RP-HPLC R_t = 13.0 min (5-60-8); biotinylated MS *m/z* calcd 2969.9 Da, found 2970.5 Da, RP-HPLC R_t = 23.0 min (5-70-30).

Peptide Apo162: MS *m/z* calcd 2692.9 Da, found 2692.6 Da, RP-HPLC R_t = 18.1 min (5-70-25); biotinylated MS *m/z* calcd 2988.9 Da, found 2987.3 Da, RP-HPLC R_t = 23.1 min (5-70-30).

Peptide Apo144-164: MS *m/z* calcd 2458.7 Da, found 2459.9 Da, RP-HPLC R_t = 16.1 min (5-70-25); biotinylated MS *m/z* calcd 2755.5 Da, found 2756.8 Da, RP-HPLC R_t = 16.5 min (5-70-25).

Peptide Apo146-164: MS *m/z* calcd 2288.5 Da, found 2288.9 Da, RP-HPLC R_t = 15.3 min (5-70-25); biotinylated MS *m/z* calcd 2586.0 Da, found 2586.0 Da, RP-HPLC R_t = 15.3 min (5-70-25).

Peptide Apo141-161: MS *m/z* calcd 2434.7 Da, found 2433.3 Da, RP-HPLC R_t = 16.8 min (5-70-25); biotinylated MS *m/z* calcd 2732.2 Da, found 2732.9 Da, RP-HPLC R_t = 16.8 min (5-70-25).

Circular Dichroism spectroscopy

Far-UV circular dichroism spectra were recorded on a J-715 spectropolarimeter (Jasco, Easton, USA), equipped with a PTC-423S/15 Peltier temperature controller, using a 0.1 cm quartz cell (Hellma, Milan, Italy) in the range 190–260 nm. Peptides (100–200 μM) were dissolved in 10 mM phosphate buffer pH 7.1 and variable volume of TFE. Spectra were acquired at 20 °C using a band width of 1 nm, a response time of 8 s, a data pitch of 0.5 nm, and a scanning speed of 10 nm/min. Each spectrum has an average of three scans with the background of the buffer solution subtracted. CD data were

expressed as molar residue ellipticity (θ). Spectra were processed using the Spectra Manager software by Jasco.

Purification of Hpt

Hpt was isolated from plasma of healthy subjects by a multi-step purification procedure, essentially according to Cigliano *et al.* [18]. Plasma proteins were fractionated by salting out in ammonium sulfate, and the protein solution was then freed of salts by gel filtration with a column of Sephacryl S-200. Fractions containing Hpt were pooled and further processed by affinity chromatography with a column of Blue Sepharose 6 Fast Flow. The column was equilibrated with P-buffer (20 mM Na_2HPO_4/ NaH_2PO_4 pH 7.0) and then loaded at 30 ml/h flow rate at room temperature. The material not retained by the resin was collected, and then the column was extensively washed with P-buffer, and finally eluted with 2 M NaCl in P-buffer. Hpt was further purified by affinity chromatography using a Sepharose resin coupled to anti-Hpt IgGs. The purity of isolated Hpt was over 98%, as assessed by SDS-PAGE and densitometric analysis of Coomassie-stained bands. The molarity of each Hpt phenotype was determined by measuring the protein concentration as mg/ml [25] and calculating the molecular weight of the monomer $\alpha\beta$ as previously described [26].

ELISA

ELISA was performed essentially as previously reported [23,27]. In particular, experiments of peptides binding to Hpt were performed incubating the wells with of 0.5 μg of Hpt in 50 μl of coating buffer (7 mM Na_2CO_3, 17 mM $NaHCO_3$, 1.5 mM NaN_3, pH 9.6). After four washes by TBS (130 mM NaCl, 20 mM Tris-HCl, pH 7.4) containing 0.05% (v/v) Tween 20 (T-TBS) and four washes by high salt TBS (500 mM NaCl in 20 mM Tris-HCl at pH 7.4), the wells were blocked with TBS (Tris-buffered saline) containing 0.5% BSA (1 h, 37 °C). The wells were then incubated with 55 μl of biotinylated peptide (0.3, 1, 3, or 10 μM). Bound peptides were then incubated (1 h at 37 °C) with 60 μl of Avidin-HRP diluted 1 : 10 000. Peroxidase-catalyzed color development from *o*-phenylenediamine was measured at 492 nm [28]. Competition experiments were performed coating the wells with 0.5 μg of HDL diluted as described earlier. A mixture of Hpt (0.9 μM) with acetylated peptides embedded into proteoliposomes (1, 5, 10, 20 or 30 μM peptide concentration) in CB-TBS buffer (5 mM $CaCl_2$, 0.2% BSA, 130 mM NaCl, 20 mM Tris-HCl, pH 7.3) was kept for 2 h at 37 °C and then incubated in the wells (2 h, 37 °C). Hpt binding was detected by treatment with 60 μl of rabbit anti-Hpt IgG (1 : 2000 dilution T-TBS containing 0.25% BSA; 1 h, 37 °C) followed by goat anti-rabbit horseradish peroxidase-conjugated-linked IgG (1 : 4000 dilution, 1 h, 37 °C). Color development was monitored at 492 nm. Absorbance values were converted to the percentage of Hpt binding in the absence of acetylated peptide.

The acetylated P2a, Apo146, and Apo157 peptides were embedded into proteoliposomes (peptide/lecithin/cholesterol, 1.5 : 200 : 18 molar ratio) prepared by the cholate dialysis technique [27]. In detail, egg lecithin in ethanol was mixed with cholesterol in ethanol, into a glass vial. The solvent was evaporated under nitrogen stream and to the dried lipids, Tris-saline (85 mM sodium cholate, 150 mM NaCl, 10 mM Tris-HCl, pH 8) was added. After vigorous whirling, the micelle suspension was incubated (90 min, 37 °C) and repeatedly shaken until clear. Then, peptide was added to the lipid suspension, which was further incubated for 1 h at 37 °C. The resulting proteoliposome suspension was extensively dialyzed against TBE (140 mM NaCl, 1 mM EDTA, 10 mM Tris–HCl, pH 7.3), at 4 °C, to remove cholate.

The molarity of Hpt (mixed phenotypes) was expressed as concentration of monomer, that is, the unit containing one subunit β (40 kDa) and one subunit α (α_1, 8.9 kDa, or α_2, 16 kDa) [10,13].

LCAT assay

A pool of plasma samples, treated with 0.65% DS (MW = 50 kDa) in 0.2 M $CaCl_2$ to remove lipoproteins, was used as source of LCAT (DS-treated plasma). The enzyme activity was measured using a proteoliposome (ApoA-I/lecithin/cholesterol = 1.5 : 200 : 8 molar contribution) as substrate, essentially according to published procedures [23]. Control assays were performed without Hpt and peptides, or in presence of Hpt. The proteoliposome was prepared by the cholate dialysis technique [29]. In detail, 8 μl of 50 mg/ml egg lecithin in ethanol were mixed with 18 μl of 1 mg/ml cholesterol in ethanol, 40 μl of [1,2-^{3}H(N)]-cholesterol (1 μCi/ml) into a glass vial. The solvent was carefully evaporated under nitrogen stream at room temperature, and to the dried lipids, 170 μl of a suspension medium (85 mM sodium cholate, 150 mM NaCl, 10 mM Tris–HCl, pH 8) was added. After vigorous whirling (3 min, room temperature), the micelle suspension was incubated (90 min, 37 °C) and repeatedly shaken every 10 min until clear. Then, 90 μl of 1.20 mg/ml ApoA-I was added to the lipid suspension, which was further incubated for 1 h at 37 °C. The resulting proteoliposome suspension was extensively dialyzed against TBE (140 mM NaCl, 1 mM EDTA, 10 mM Tris–HCl, pH 7.3), at 4 °C, to remove cholate. The dialyzed volume was adjusted to 285 μl using TBE. The reaction mixture (1 ml final volume) was prepared by putting together 697 μl of TBE containing 5 mM $CaCl_2$, 83 μl of 6% human serum albumin, and 160 μl of proteoliposome suspension (diluted 1 : 20 in TBE) into a screw-capped tube and heating at 38 °C for 30 min. The assay was carried out by addition of 2.5 μl of 2 mM β-mercaptoethanol and 3.5 μl of DS-treated plasma to 100 μl of reaction mixture, which was rapidly divided into three aliquots of 32 μl and incubated (1 h, 37 °C). The reaction was stopped by addition of 130 μl of ethanol to each aliquot. The lipids were extracted in 600 μl of hexane, containing 10 μg/ml cholesterol and 10 μg/ml cholesteryl linoleate. After recovering the organic phase, the aqueous phase was again treated with 500 μl of the extraction solution (twice), and the three extracts were pooled. Hexane was removed under nitrogen stream, and the dried lipids were dissolved in 50 μl of chloroform. Cholesteryl esters were separated from cholesterol by thin layer chromatography, using petroleum ether, diethyl ether, and acetic acid (90 : 30 : 1, v : v : v) as mobile phase. The lipid spots were visualized under iodine vapor and recovered for scintillation analysis. The enzyme activity was expressed in units (nmol of cholesterol esterified/h/ ml of plasma).

Statistical Analysis

ELISA was carried out with three replicates. Samples in the LCAT assay were analyzed in triplicate. The data were expressed as mean value ± SEM. The program GraphPad Prism 5.01 (GraphPad Software, San Diego, CA, USA) was used to evaluate significance of statistical differences by one-way ANOVA, followed by Tukey's test for multiple comparisons.

Results and Discussion

Peptides Design and Synthesis

In order to identify the P2a residues involved in Hpt recognition, we designed a series of P2a analogs by varying the peptide length or by

Journal of PeptideScience

introducing single point mutations. In particular, peptide P2a sequence, which reproduces ApoA-I 141–164 region, contains eight charged residues and two histidines that are highly conserved between species (Figure 1). We singularly replaced each of these residues with alanine, in order to evaluate the contribution of the side-chains to the binding to Hpt (Table 1). Furthermore, P2a was truncated at both terminal sides to evaluate the minimal sequence requirements for its bioactivity (Table 2).

Binding Analysis of P2a Analog Peptides to Hpt

In order to evaluate the minimal P2a sequence required for Hpt binding, different amounts (0.3, 1, 3 or 10 μM) of biotinylated truncated peptides (Apo141-161, Apo144-164, and Apo146-164) were loaded into Hpt-coated wells, and their efficiency of binding to Hpt was compared with that of P2a by ELISA. As shown in Figure 2 (A), the peptide Apo144-164 bound Hpt with efficiency similar to that of P2a, when used at 0.3 or 1 μM concentration and higher than P2a ($p < 0.01$) when used at 3 or 10 μM concentration. The deletion of two more residues at the *N*-terminal of P2a (Apo146-164) resulted in an evident drop of binding efficiency with respect to P2a at all the assayed concentration. The *C*-terminal truncated peptide Apo141-161 exhibited a binding efficiency lower than P2a ($p < 0.01$) in the range 0.3–3 μM and similar to P2a when used at 10 μM concentration. These results suggest that the ApoA-I sequence 144–164 is essential for the binding to Hpt.

In order to assess the Hpt binding contribution of charged and histidine residues, ten conserved residues were replaced with alanine (Table 1). The biotinylated peptides were separately incubated in Hpt-coated wells and Avidin-HRP was used to detect their binding to Hpt. The analysis of the peptide binding to Hpt showed that replacement with alanine is not detrimental. In particular, the peptides with Glu146Ala (Apo146), Asp157Ala (Apo157), or His162Ala (Apo162) substitutions showed a binding efficiency to Hpt significantly higher ($p < 0.01$) than P2a, at any concentration used in the assay [Figure 2(B)]. Notably, this effect was dose-dependent.

The results of the binding experiments suggest that charged and histidine residues are not involved in Hpt recognition, and hydrophobic interactions play a major role in driving the binding. The increase in binding efficiency of Apo146 and Apo157 peptides could reflect the elimination of an unfavorable electrostatic interaction or the stabilization of a more favorable conformation. Indeed, amino acids

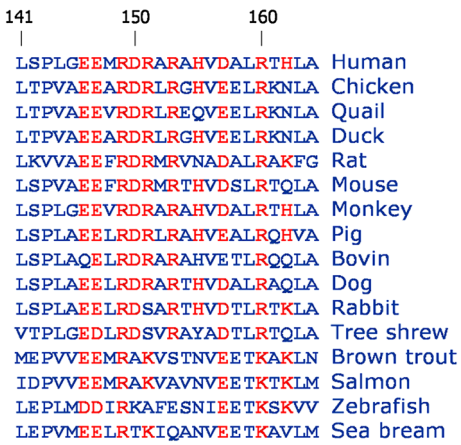

Figure 1. Sequence alignment of ApoA-I 141–164 region from different sources. Charged and histidine residues are highlighted in red.

Table 1. Amino acid sequence of P2a and alanine substituted analogs

Peptide	Sequence
P2a	Ac–LSPLGEEMRDRARAHVDALRTHLA–NH_2
Apo146	Ac–LSPLG**A**EMRDRARAHVDALRTHLA–NH_2
Apo147	Ac–LSPLGE**A**MRDRARAHVDALRTHLA–NH_2
Apo149	Ac–LSPLGEEM**A**DRARAHVDALRTHLA–NH_2
Apo150	Ac–LSPLGEEMR**A**RARAHVDALRTHLA–NH_2
Apo151	Ac–LSPLGEEMRD**A**ARAHVDALRTHLA–NH_2
Apo153	Ac–LSPLGEEMRDRA**A**AHVDALRTHLA–NH_2
Apo155	Ac–LSPLGEEMRDRARA**A**VDALRTHLA–NH_2
Apo157	Ac–LSPLGEEMRDRARAHV**A**ALRTHLA–NH_2
Apo160	Ac–LSPLGEEMRDRARAHVDAL**A**THLA–NH_2
Apo162	Ac–LSPLGEEMRDRARAHVDALRT**A**LA–NH_2

replacement with alanine, which has the highest intrinsic helix propensity [30], may affect peptide helix content. The change in binding efficiency could reflect a different ability of the peptide to adopt the helical conformation in solution or when bound to Hpt, as ApoA-I region 141–164 assumes a helical conformation in the native protein.

Far-UV Circular Dichroism Analysis

The conformational properties of peptide P2a and its alanine analogs were investigated by far-UV circular dichroism spectroscopy to evaluate their propensity to adopt a helical secondary structure. The CD spectra of peptides in phosphate buffer (Figure 3) are characterized by a deep minimum around 200 nm and shallow minimum centered at 222 nm. These spectra indicate that all the analyzed peptides are predominantly in a random coil conformation with a small percentage of helical structure in water solution. This result is not surprising considering that amino acid sequences excised from their natural context rarely adopt in water solution the native conformation. In order to verify peptides propensity toward a helical conformation, we performed a titration with TFE, a well-known organic cosolvent able to stabilize a helical conformation in peptides [31]. CD spectra of peptides were acquired increasing TFE volume from 0% to 50% as it is well known that the TFE reaches its stabilizing effect around the percentage of 40% of volume [32].

Increasing TFE volume all peptide spectra (Figure 3) showed a shift toward 208 nm and an increase of intensity of the minimum at lower wavelength; contemporary, the intensity of the band at 222 nm significantly increased. A crossover (around 200 nm) and an isodichroic (at 203 nm) points were revealed in all titrations. The ratio of ellipticity at 222 (θ_{222}) and 208 nm (θ_{208}) was around the unity at 40% TFE for all peptides [33]. Furthermore, all peptides showed a sigmoidal-like variation of the helical induction curve (data not shown). These spectral characteristics are clearly indicative of a transition from a random coil to an α-helical conformation. CD

Table 2. Amino acid sequence of truncated P2a peptides

Peptide	Sequence
P2a	Ac–LSPLGEEMRDRARAHVDALRTHLA–NH_2
Apo144-164	Ac–LGEEMRDRARAHVDALRTHLA–NH_2
Apo146-164	Ac–EEMRDRARAHVDALRTHLA–NH_2
Apo141-161	Ac–LSPLGEEMRDRARAHVDALRT–NH_2

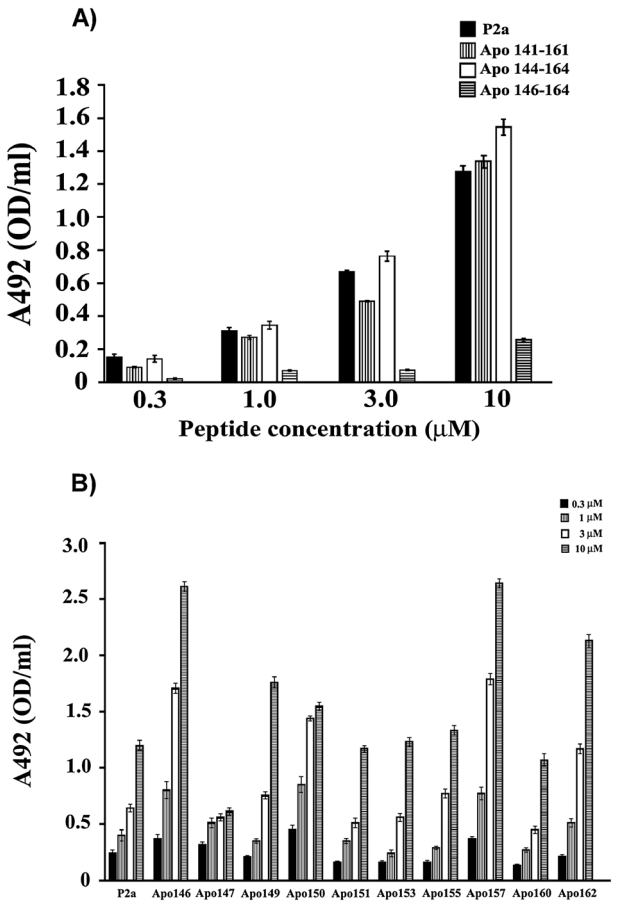

Figure 2. Binding of truncated (A) and P2a analogs (B) to Hpt. Different concentrations (0.3, 1, 3, or 10 μM) of biotinylated peptides were incubated in Hpt-coated wells. Avidin-HRP was used to detect bound peptides. The samples were analyzed in triplicate and the data are expressed as mean ± SEM.

spectra of peptides in presence of 20% TFE almost showed the full characteristics of a helical conformation.

Analysis of the TFE titration experiments showed that, although in all analyzed peptides, the helical conformation is scarcely populated in water solution, all peptide analogs are able to assume a helical conformation in a water/TFE solution. On the basis of CD experiments, we can conclude that alanine replacement does not significantly modify the conformational properties of P2a peptide analogs; hence, the different Hpt binding efficiency should be attributed to side-chain replacement. In particular, all P2a analogs showed a comparable binding efficiency with respect to P2a except for Apo146 and Apo157 peptides. We can speculate that when P2a binds to Hpt, it localizes the side chain of Glu146 and Asp157 close to two negative charged regions that interact unfavorable with Glu146 and Asp157 side chains.

Competition of Peptides (P2a, Apo146, and Apo157) with HDL for Binding Hpt

In order to investigate the biological properties of the two P2a analogs with the highest Hpt binding efficiency (Apo146 and Apo157), the ability of Apo146 and Apo157 to influence the Hpt binding to HDL was evaluated *in vitro* and compared with that of P2a. HDL-coated wells were incubated with Hpt in the absence or presence of different amounts (1–30 μM) of each acetylated peptide (P2a, Apo146, or Apo157), and the amount of HDL-bound Hpt was measured. The three peptides, at concentration higher than 1 μM, significantly impaired Hpt binding to HDL ($p < 0.0001$). Interestingly, the inhibition of Hpt binding to HDL by Apo157 was higher than those of P2a and Apo146, at any assayed concentration ($p < 0.0001$). In particular, as shown in Figure 4, P2a and Apo146 displaced up to about 55% of Hpt from binding HDL ($p < 0.0001$), with no difference between them, at any assayed concentration, whereas the peptide Apo157 was able to displace up to 65% of Hpt ($p < 0.0001$). These

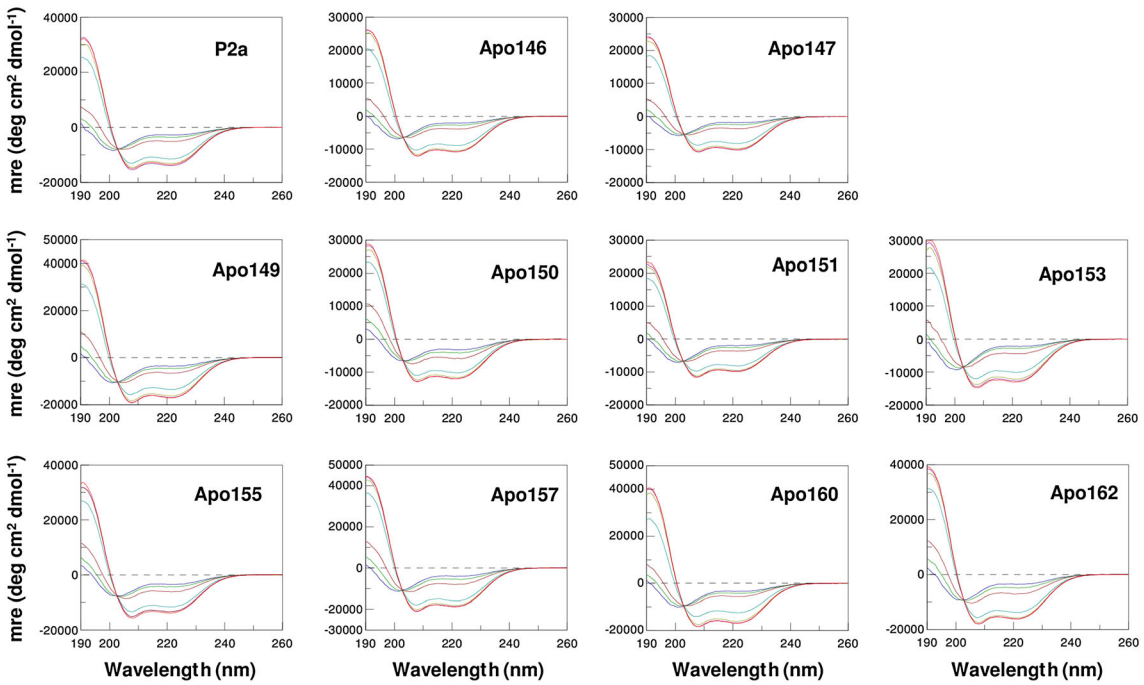

Figure 3. Far-UV circular discroism analysis of P2a analogs. TFE titration spectra of P2a peptide analogs were acquired at 20 °C in 10 mM phosphate buffer with increasing volume of TFE from 0% to 50%. Spectra are reported as molar residue ellipticity.

Journal of PeptideScience

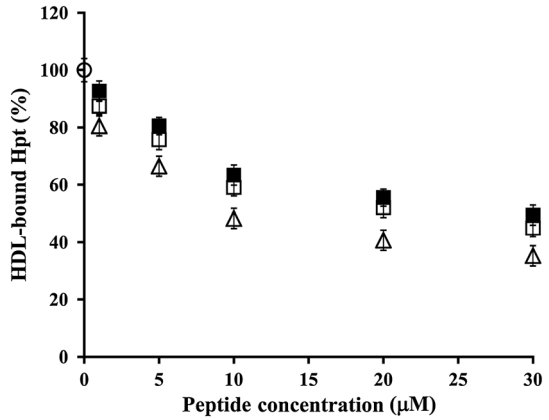

Figure 4. Peptide competition with HDL for binding Hpt. Hpt (0.9 μM) was incubated for 2 h at 37 °C with acetylated P2a (full squares), or Apo146 (open squares) or Apo157 (open triangles) (0–30 μM). Aliquots were then incubated in HDL-coated wells (2 h, 37 °C). Hpt binding to HDL was detected by rabbit anti-Hpt IgG and GAR-HRP IgG. The amount of immunocomplexes was determined by measuring the absorbance at 492 nm. Data are reported as percent of the value obtained by incubation of Hpt alone (open circle) and expressed as mean ± SEM.

results suggest that the Asp157Ala substitution in the P2a sequence improves the binding of the peptide to Hpt.

LCAT Inhibition by Hpt: Effect of P2a or Apo146 or Apo157

The ability of the peptides to compete with ApoA-I for binding Hpt was also evaluated in LCAT activity assay. DS-treated plasma and labeled proteoliposomes (LCAT and ApoA-I-containing cholesterol sources, respectively) were incubated with 0.4 μM Hpt, in the absence or presence of different amounts (0.8 or 1.2 μM) of each peptide. The LCAT activity was significantly reduced (about 74%) by Hpt (5.42 ± 0.12 units versus 1.47 ± 0.02 units; $p < 0.0001$) but differently restored when peptides were present during incubation (Figure 5), with Apo146 and Apo157 being more effective than P2a ($p < 0.0001$) in rescuing the enzyme activity. In particular, the use

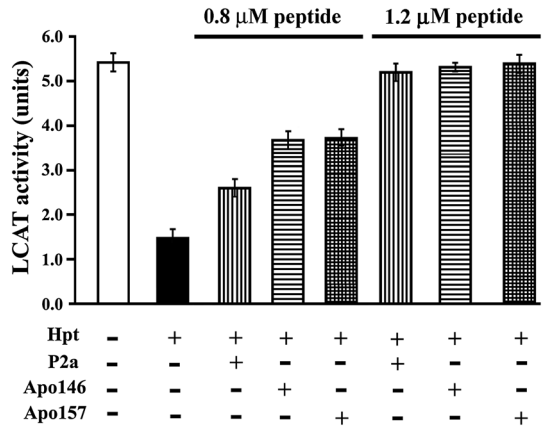

Figure 5. Effect of peptides on the inhibition of LCAT activity by Hpt. The LCAT activity was assayed in absence or presence of 0.4 μM Hpt and different amounts (0.8 or 1.2 μM) of P2a or Apo146 or Apo157. A pool of plasma samples (treated with 0.65% dextran sulfate, MW = 50 kDa, in 0.2 M $CaCl_2$ to remove lipoproteins) was used as source of LCAT, whereas a proteoliposome (ApoA-I/lecithin/^{3}H-cholesterol, 1.5 : 200 : 18 molar ratio) was used as substrate. The LCAT activity is expressed in units corresponding to nmol of cholesterol incorporated per hour per ml of plasma. Samples were analyzed in triplicate, and data are expressed as means ± SEM.

of 0.8 μM (peptide/Hpt molar ratio 2:1) of Apo146 or Apo157 in the assay restored about 70% of the LCAT activity, with no difference between the two peptides, whereas P2a, at this concentration, restored 50% of the LCAT activity, thus confirming that amino acid changes in P2a sequence influence the affinity of the peptide for Hpt. The three peptides fully saved the enzyme stimulation by ApoA-I, when used at 1.2 μM concentration in the assay (peptide/Hpt molar ratio 4 : 1). The peptides, when incubated without Hpt, did not significantly affect the cholesterol esterification (data not shown).

Conclusions

P2a peptide sequence was modified in order to analyze the molecular determinants of Hpt binding. Analysis of truncated P2a analogs showed that P2a sequence can only be slightly reduced in length at the *N*-terminal, without altering the ability of binding to Hpt. In particular, the deletion of the dipeptide Leu144-Gly145 drastically reduces the binding to Hpt, suggesting an important role of hydrophobic interactions. Furthermore, the role of charged residues was systematically analyzed by replacing them with alanine. Binding assays showed that charged residues are not involved in Hpt recognition; actually, E146A e D157A substitutions increase the binding affinity to Hpt. Biological characterization of the corresponding P2a peptide analogs, Apo146 and Apo157, showed that the two peptides are more effective than P2a in rescuing the LCAT activity from Hpt inhibition. This result suggests novel hints to design peptides with anti-atherogenic activity, which, displacing Hpt from HDL, might rescue LCAT activity and improve reverse cholesterol transport.

References

1 Sorci-Thomas MG, Thomas MJ. The effects of altered apolipoprotein A-I structure on plasma HDL concentration. *Trends Cardiovasc. Med.* 2002; **12**: 121–128.
2 Davidson WS, Thompson TB. The structure of apolipoprotein A-I in high density lipoproteins. *J. Biol. Chem.* 2007; **282**: 22249–22253.
3 Thomas MJ, Bhat S, Sorci-Thomas MG. Three-dimensional models of HDL apoA-I: implications for its assembly and function. *J. Lipid Res.* 2008; **49**: 1875–1883.
4 Wu Z, Gogonea V, Lee X, Wagner MA, Li XM, Huang Y, Undurti A, May RP, Haertlein M, Moulin M, Gutsche I, Zaccai G, Didonato JA and Hazen SL. Double superhelix model of high density lipoprotein. *J. Biol. Chem.* 2009; **284**: 36605–36619.
5 Mei X, Atkinson D. Crystal structure of *C*-terminal truncated apolipoprotein A-I reveals the assembly of high density lipoprotein (HDL) by dimerization. *J. Biol. Chem.* 2011; **286**: 38570–38582.
6 Huang R, Silva RA, Jerome WG, Kontush A, Chapman MJ, Curtiss LK, Hodges TJ, Davidson WS. Apolipoprotein A-I structural organization in high-density lipoproteins isolated from human plasma. *Nat. Struct. Mol. Biol.* 2011; **18**: 416–422.
7 Wu Z, Gogonea V, Lee X, May RP, Pipich V, Wagner MA, Undurti A, Tallant TC, Baleanu-Gogonea C, Charlton F, Ioffe A, Di Donato JA, Rye KA, Hazen SL. The low resolution structure of ApoA1 in spherical high density lipoprotein revealed by small angle neutron scattering. *J. Biol. Chem.* 2011; **286**: 12495–124508.
8 Sevugan Chetty P, Mayne L, Kan ZY, Lund-Katz S, Englander SW, Phillips MC Apolipoprotein A-I helical structure and stability in discoidal high-density lipoprotein (HDL) particles by hydrogen exchange and mass spectrometry. *Proc. Natl. Acad. Sci. U.S.A.* 2012; **109**: 11687–11692.
9 Balestrieri M, Cigliano L, De Simone ML, Dale B, Abrescia P. Haptoglobin inhibits lecithin-cholesterol-acyltrasferase in human ovarian follicular fluid. *Mol. Reprod. Dev.* 2001; **59**: 186–191.
10 Spagnuolo MS, Cigliano L, Abrescia, P. The binding of haptoglobin to apolipoprotein A-I: influence of hemoglobin and concanavalin A. *Biol. Chem.* 2003; **384**: 1593–1596.

11 Giblett ER. The haptoglobin system. *Ser. Haematol.* 1968; **1**: 3–20.
12 Nagel RL, Gibson QH. The binding of Hemoglobin to Haptoglobin and its relation to subunit dissociation of Hemoglobin. *J. Biol. Chem.* 1971, **246**: 69–73.
13 Langlois MR, Delanghe JR. Biological and clinical significance of haptoglobin polymorphism in humans. *Clin. Chem.* 1996; **42**: 1589–1600.
14 Kristiansen M, Graversen JH, Jacobsen C, Sonne O, Hoffman HJ, Law SK, Moestrup SK Identification of the haemoglobin scavenger receptor. *Nature* 2001; **409**: 198–201.
15 Gutteridge JMC. The antioxidant activity of haptoglobin towards haemoglobin-stimulated lipid peroxidation. *Biochim. Biophys. Acta* 1987; **917**: 219–223.
16 Alayash AI. Redox biology of blood. *Antioxid. Redox Signal.* 2004; **6**: 941–949.
17 Salvatore A, Cigliano L, Bucci EM, Corpillo D, Velasco S, Carlucci A, Pedone C, Abrescia P. Haptoglobin binding to apolipoprotein A-I prevents damage from hydroxyl radicals on its stimulatory activity of the enzyme lecithin-cholesterol acyl-transferase. *Biochemistry* 2007; **46**: 1158–1168.
18 Cigliano L, Pugliese CR, Spagnuolo MS, Palumbo R, Abrescia P. Haptoglobin binds the antiatherogenic protein apolipoprotein E - impairment of apolipoprotein E stimulation of both lecithin: cholesterol acyltransferase activity and cholesterol uptake by hepatocytes. *FEBS J.* 2009; **276**: 6158–6171.
19 Braeckman L, De Bacquer D, Delanghe J, Claeys L, De Backer G. Associations between haptoglobin polymorphism, lipids, lipoproteins and inflammatory variables. *Atherosclerosis* 1999; **143**: 383–388.
20 De Bacquer D, De Backer G, Langlois M, Delanghe J, Kesteloot H, Kornitzer M. Haptoglobin polymorphism as a risk factor for coronary heart disease mortality. *Atherosclerosis* 2001; **157**: 161–166.
21 Matuszek MA, Aristoteli LP, Bannon PG, Hendel PN, Hughes CF, Jessup W, Dean RT, Kritharides L. Haptoglobin elutes from human atherosclerotic coronary arteries--a potential marker of arterial pathology. *Atherosclerosis* 2003; **168**: 389–396.
22 Sorci-Thomas MG, Curtiss L, Parks JS, Thomas MJ, Kearns MW, Landrum M. The hydrophobic face orientation of apolipoprotein A-I amphipathic helix domain 143–164 regulates lecithin: cholesterol acyltransferase activation. *J. Biol. Chem.* 1998; **273**: 11776–11782.
23 Spagnuolo MS, Cigliano L, D'Andrea LD, Pedone C, Abrescia P Assignment of the binding site for haptoglobin on apolipoprotein A-I. *J. Biol. Chem.* 2005; **280**: 1193–1198.
24 Bucci M, Cigliano L, Vellecco V, D'Andrea LD, Ziaco B, Rossi A, Sautebin L, Carlucci A, Abrescia P, Pedone C, Ianaro A, Cirino G. Apolipoprotein A-I (ApoA-I) mimetic peptide P2a by restoring cholesterol esterification unmasks ApoA-I anti-inflammatory endogenous activity *in vivo*. *J. Pharmacol. Exp. Ther.* 2012; **340**: 716–722.
25 Bradford MM. A rapid and sensitive method for the quantitation of microgram quantities of protein utilizing the principle of protein-dye binding. *Anal. Biochem.* 1976; **72**: 248–254.
26 Cigliano L, Spagnuolo MS, Abrescia P Quantitative variations of the isoforms in haptoglobin 1-2 and 2-2 individual phenotypes. *Arch. Biochem. Biophys.* 2003; **416**: 227–237.
27 Cigliano L, D'Andrea LD, Maresca B, Serino M, Carlucci A, Salvatore A, Spagnuolo MS, Scigliuolo G, Pedone C, Abrescia P. Relevance of the amino acid conversions L144R (Zaragoza) and L159P (Zavalla) in the apolipoprotein A-I binding site for haptoglobin. *Biol. Chem.* 2008; **389**: 1421–1426.
28 Porta A, Cassano E, Balestrieri M, Bianco M, Picone R, De Stefano C, Abrescia P. Haptoglobin transport into human ovarian follicles and its binding to apolipoprotein A-I. *Zygote* 1999; **7**: 67–77.
29 Chen C-H, Albers JJ. Characterization of proteoliposomes containing apoprotein A-I: a new substrate for the measurement of lecithin: cholesterol acyltransferase activity. *J. Lipid Res.* 1982; **23**: 680–691.
30 DeGrado WF, Summa CM, Pavone V, Nastri F, Lombardi A. De novo design and structural characterization of proteins and metalloproteins. *Annu. Rev. Biochem.* 1999; **68**: 779–819.
31 Luo P, Baldwin RL. Mechanism of helix induction by trifluoroethanol: a framework for extrapolating the helix-forming properties of peptides from trifluoroethanol/water mixtures back to water. *Biochemistry* 1997; **36**: 8413–8421.
32 Rohl CA, Chakrabartty A, Baldwin RL Helix propagation and N-cap propensities of the amino acids measured in alanine-based peptides in 40 volume percent trifluoroethanol. *Protein Sci.* 1996; **5**: 2623–2637.
33 Vuilleumier S, Mutter M. Synthetic peptide and template-assembled synthetic protein models of the hen egg white lysozyme 87–97 helix: importance of a protein-like framework for conformational stability in a short peptide sequence. *Biopolymers* 1993; **33**: 389–400.

